Non-smooth modelling of electrical systems using the flux approach

Michael Möller · Christoph Glocker

Abstract The non-smooth modelling of electrical systems, which allows for idealised switching components, is described using the flux approach. The formulations and assumptions used for non-smooth mechanical systems are adopted for electrical systems using the position–flux analogy. For the most important non-smooth electrical elements, like diodes and switches, set-valued branch relations are formulated and related to analogous mechanical elements. With the set-valued branch relations, the dynamics of electrical circuits are described as measure differential inclusions. For the numerical solution, the measure differential inclusions are formulated as a measure complementarity system and discretised with a difference scheme, known in mechanics as time-stepping. For every time-step a linear complementarity problem is obtained. Using the example of the DC–DC buck converter, the formulation of the measure differential inclusions, state reduction and their numerical solution using the time-stepping method is shown for the flux approach.

Keywords Non-smooth · Ideal · Diode · Switch · Complementarity · Discontinuity

M. Möller (✉) · Ch. Glocker
IMES, Center of Mechanics, ETH Zurich, CH-8092
Zurich, Switzerland
e-mail: michael.moeller@imes.mavt.ethz.ch

1 Introduction

A good model only describes the relevant physical effects of a real device with respect to a certain application problem. This includes that the model contains only dynamics at the relevant time scale and high frequency dynamics is therefore neglected as much as possible. Sometimes not all high frequency dynamics can be removed from the model, since it may be essential for the device to work. For some applications, the exact high frequency dynamical behaviour can be replaced by discontinuity events, which contain all the non-negligible details of the high frequency dynamics in a simplified form, while preserving the essential behaviour of the device. For electrical systems this means that elements like switches and diodes are modeled as ideal non-smooth elements instead of nonlinear regularised elements.

There exist well-developed analytical formulations and numerical methods for non-smooth mechanical systems, pioneered by the work of Moreau [17], allowing for ideal unilateral contacts and friction. In [13], the idealised modelling of switches and diodes in the charge approach is introduced and linked to non-smooth mechanics. The dynamical behaviour is formulated as a differential inclusion and solved numerically using the time-stepping method. A method for the modelling of electro-mechanical systems with variable structure in the electrical subsystem is presented in [10] with the focus on the diode. In the charge approach for electrical systems, the currents and

charges are used as variables. In contrast, the flux approach uses the voltages and fluxes as variables. The aim of this paper is to extend the flux approach to non-smooth electrical systems. The electro-mechanical analogy will be used to link the electrical models in the flux approach to mechanical models. The assumptions and formulations used for non-smooth mechanical systems in the position approach will be adopted for electrical systems in the flux approach using the electro-mechanical analogy. As in mechanics and in the charge approach, the time-stepping method will be used for the numerical solution of the differential inclusion obtained using the flux approach. The DC–DC buck converter will be used as an example circuit.

Much fundamental work has already been done on the modelling, the analysis and the control of electrical networks. In particular, anomalous bifurcation behaviour has drawn the attention of many researchers to electronic power converters, in which a special type of non-smooth bifurcation has been observed. In the seminal work of [4] and [5], this type has been called border collision bifurcation and has been investigated in great detail in the form of case studies not only for DC–DC buck and boost converters [5], but also theoretically [4] to provide analytical explanations of borderline collisions. In contrast to [4] and [5], in which standard models of the converters are used, the groundbreaking theoretical and experimental work [15] suggests a buck converter model on a level of sophistication, in which also parasitics elements are included. Rich bifurcation scenarios are revealed by numerical analysis and confirmed by experiments. Boost converters are treated in the papers [16] and [20].

As soon as the model of an electrical circuit has been drawn as a circuit diagram, it is quite clear on how to obtain its governing equations. If the circuit contains switching elements such as diodes or the like, one usually writes down the governing equations for each state of operation separately, and completes them by adequate state transition rules. This procedure reflects the today's state of the art in the modelling of switched networks and has also been applied in all contributions cited in the previous paragraph. By this method, non-accessible topologies are often excluded from the analysis in a heuristic manner in order to reduce the number of states that have to be considered. This approach, however, is restricted to circuits with a small number of switching elements only, because the administrative overhead to implement such kind of transition rules and to keep track of all possible cases becomes enormous. All those difficulties are known within the community. We refer, in particular, to [6], in which a full list of such problems has been stated. In contrast, the paper at hand as well as [13] suggests to treat diodes and switches as circuit elements, equipped with (set-valued) branch relations that intrinsically carry both, the different states of the elements and the state transition rules. By this approach, the Filippov-type differential inclusions of the associated circuits are generated in a very natural manner by just the elements themselves, and no additional convexification concept is needed. This approach has proven to be successful up to ten thousands of non-smooth elements.

We do not intend to discuss the rich nonlinear behaviour of the converter, because this has already been done at other places. We have chosen the DC–DC buck converter as a well-known example on which to demonstrate non-smooth modelling by using the flux approach. The same example has been treated in [13] by using the charge approach. This allows for a comparison of the two dual approaches not only on an abstract basis but on an example circuit as well. With respect to the presented time-stepping scheme, the most degenerated version of the DC–DC buck converter is the most demanding one. We therefore discuss two versions of the buck converter: The first one is an extended model that takes into account some parasitics in the spirit of [15], leading to a system that complies with Lagrangian mechanics. The second one is the standard model [5], which differs from Lagrangian mechanics by a degenerated capacitor matrix. Due to its implicit nature, our time-stepping approach is able to handle even the degenerated standard model, which is demonstrated in Section 5. For completeness, the full MATLAB® implementation is provided, allowing for a direct reproduction of the numerical results on the one hand, and for illustrating the compactness and simplicity of code on the other hand.

The most basic set-valued elements are summarised in Section 2, while Section 3 gives an overview of the different analogous mechanical and electrical descriptions. In Section 4, the flux approach for classical and non-smooth electrical systems is described. The theories presented in Section 4 are then applied to the DC–DC buck converter in Section 5.

Fig. 1 The maps
$x \rightarrow \mathrm{Upr}(x)$ and
$x \rightarrow \mathrm{Upr}^{-1}(x)$
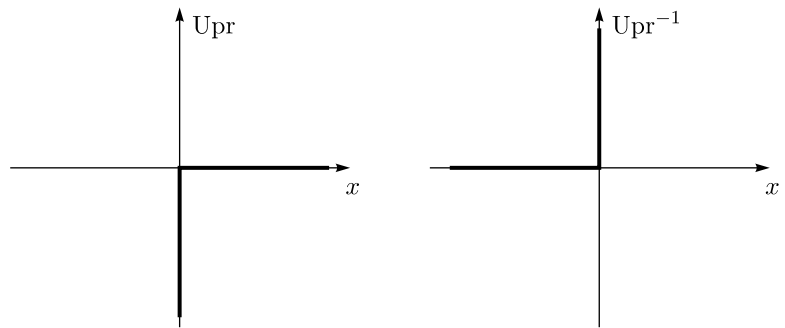
2 Set-valued elements

In this section, the most important set-valued elements, together with some relations needed in the following sections, are summarised. In Section 2.1, the linear complementarity problem is described. The set-valued elements described in Sections 2.2 and 2.3 are used to formulate the constitutive laws for the non-smooth elements.

2.1 The linear complementarity problem

A linear complementarity problem (LCP) can be formulated as a problem of the following form [7]: For a given matrix $A \in \mathbb{R}^{n,n}$ and a vector $b \in \mathbb{R}^n$, find the vectors $x \in \mathbb{R}^n$ and $y \in \mathbb{R}^n$ such that the linear equation $y = Ax + b$ holds together with the complementarity conditions $y_i \geq 0$, $x_i \geq 0$, $y_i x_i = 0$ for $i = 1, \ldots, n$. Very often an LCP is written as

$$y = Ax + b, \quad 0 \preceq y \perp x \succeq 0. \tag{1}$$

An LCP can be solved by enumerating all combinations of x_i and y_i that satisfy the complementarity condition $y_i x_i = 0$. For every i, there are the two possibilities that either $y_i \geq 0$ and $x_i = 0$ or $y_i = 0$ and $x_i \geq 0$. Since the vectors have n components there are 2^n cases, and for each a linear system of equations has to be solved. An LCP can have a unique solution, multiple solutions or no solution at all. The enumerative methods are very inefficient for large LCPs, because the number 2^n of linear systems that has to be solved grows rapidly. More efficient algorithms to solve an LCP can be found in [7].

2.2 The unilateral primitive

The unilateral primitive Upr is a maximal monotone set-valued map on $\mathbb{R}^+$ defined by

$$\mathrm{Upr}(x) := \begin{cases} \{0\}, & x > 0 \\ (-\infty, 0], & x = 0 \end{cases}. \tag{2}$$

The graph of this map is depicted in Fig. 1. Each complementarity condition of an LCP can be expressed as one Upr inclusion

$$-y \in \mathrm{Upr}(x) \Leftrightarrow y \geq 0, \quad x \geq 0, \quad xy = 0. \tag{3}$$

Since the complementarity condition is symmetric in x and y the following inclusions are equivalent:

$$-y \in \mathrm{Upr}(x) \Leftrightarrow -x \in \mathrm{Upr}(y). \tag{4}$$

From this equivalence follows directly the relation

$$\mathrm{Upr}^{-1}(-y) = -\mathrm{Upr}(y) \tag{5}$$

for the inverse Upr^{-1} of the maximal monotone map Upr (cf. Fig. 1). The unilateral primitive is invariant under scaling with positive values
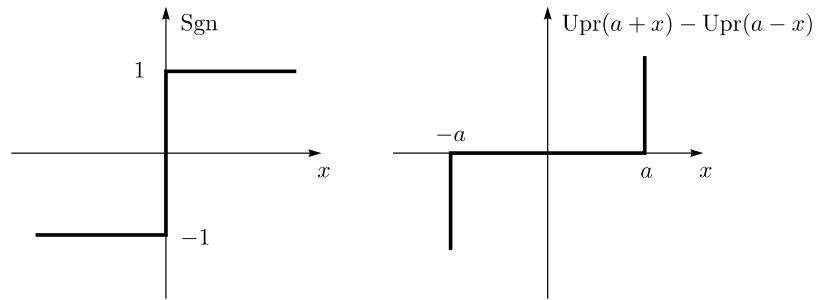
$$\forall a > 0: \quad \mathrm{Upr}(ax) = \mathrm{Upr}(x), \tag{6}$$

$$\forall a > 0: \quad a \cdot \mathrm{Upr}(x) = \mathrm{Upr}(x). \tag{7}$$

The addition of two unilateral primitives results again in a unilateral primitive

$$\mathrm{Upr}(x) + \mathrm{Upr}(x - a) = \mathrm{Upr}(x - b)$$

$$\text{with } b = \max(0, a). \tag{8}$$

Fig. 2 The maps $x \to \mathrm{Sgn}(x)$ and $x \to \mathrm{Upr}(a+x) - \mathrm{Upr}(a-x)$

2.3 The Sgn-multifunction

The Sgn-multifunction is a maximal monotone set-valued map defined by

$$\mathrm{Sgn}\,(x) := \begin{cases} \{1\}, & x > 0 \\ [-1, 1], & x = 0 \\ \{-1\}, & x < 0 \end{cases}. \tag{9}$$

While the classical sgn-function is defined with $\mathrm{sgn}(0) = 0$, the Sgn-multifunction is set-valued at $x = 0$. The graph of the Sgn-multifunction is depicted in Fig. 2. An inclusion in the Sgn-multifunction can always be represented by two inclusions involving the unilateral primitive. The decomposition may be written as

$$\forall a \geq 0 : -y \in a \cdot \mathrm{Sgn}(x)$$
$$\Leftrightarrow \exists\, x_R, x_L \text{ such that } \begin{cases} -y \in +\mathrm{Upr}(x_R) + a \\ -y \in -\mathrm{Upr}(x_L) - a \\ x = x_R - x_L \end{cases} \tag{10}$$

The unilateral primitive on the right side of Equation (10) can be inverted by using the relation (4), which yields

$$\forall a \geq 0 : -y \in a \cdot \mathrm{Sgn}(x)$$
$$\Leftrightarrow \exists\, x_R, x_L \text{ such that } \begin{cases} -x_R \in \mathrm{Upr}(a + y) \\ -x_L \in \mathrm{Upr}(a - y) \\ x = x_R - x_L \end{cases} \tag{11}$$

By eliminating the variables x_R and x_L one obtains the relation

$$\forall a \geq 0 : -y \in a \cdot \mathrm{Sgn}(x)$$
$$\Leftrightarrow -x \in \mathrm{Upr}(a + y) - \mathrm{Upr}(a - y) \tag{12}$$

for the inverse map of the Sgn-multifunction. The map $x \to \mathrm{Upr}(a + x) - \mathrm{Upr}(a - x)$, as depicted in Fig. 2, can be written as

$$\forall a \geq 0 : \ \mathrm{Upr}(a + x) - \mathrm{Upr}(a - x)$$
$$= \begin{cases} (-\infty, 0], & x = -a \\ \{0\}, & -a < x < a \\ [0, \infty), & x = a \end{cases}. \tag{13}$$

3 Electro-mechanical analogy

In this section, an overview of four analogous models of dynamic mechanical and electrical systems is given. For the mechanical and the electrical systems, only lumped parameter models are considered, i.e. the electrical networks consist only of abstract 2-poles and idealised wires while the mechanical systems contain no continua. The lumped parameter assumption allows us to describe the dynamics of the system with a set of differential equations for smooth motion and a set of measure differential inclusions for non-smooth motion. Partial differential equations are therefore not considered. The mechanical models are restricted to models with linear kinematics, in order to keep the analogy between mechanical and electrical systems as simple as possible. In Section 3.1, the classical analogy for smooth mechanical and electrical systems is described. The analogy for non-smooth systems is discussed in Section 3.2. The analogy between the position approach in mechanics and the charge approach in electronics has been described in [13] for classical and non-smooth systems.

3.1 Classical analogy

In mechanics, usually the positions $r(t)$ with the associated velocities $v(t)$ are chosen as independent

Table 1 Corresponding variables and elements in mechanics and electronics

	Mechanics position app.	Mechanics momentum app.	Electronics charge approach	Electronics flux approach
Local variables	Position $r(t)$	Momentum $p(t)$	Charge $g(t)$	Flux $\varphi(t)$
	Velocity $v(t)$	Force $f(t)$	Current $\iota(t)$	Voltage $u(t)$
	Force $f(t)$	Velocity $v(t)$	Voltage $u(t)$	Current $\iota(t)$
Inertia	Mass m	Stiffness k	Inductivity L	Capacity C
	$f = -m\dot{v}$	$v = -\frac{1}{k}\dot{f}$	$u = -Li$	$\iota = -C\dot{u}$
Dissipation	Damping d	Damping d	Resistance R	Resistance R
	$f = -dv$	$v = -\frac{1}{d}f$	$u = -R\iota$	$\iota = -\frac{1}{R}u$
Energy storage	Stiffness k	Mass m	Capacity C	Inductivity L
	$f = -kr$	$v = -\frac{1}{m}p$	$u = -\frac{1}{C}g$	$\iota = -\frac{1}{L}\varphi$

variables

$$r(t) = r(t_0) + \int_{t_0}^{t} v(\tau)\,\mathrm{d}\tau. \tag{14}$$

The three classical elements are the mass m, the damping d and the stiffness k (cf. Table 1). For electrical systems there are three common approaches to describe the dynamics of the system: The charge approach, the flux approach and mixed approaches [10]. In the charge approach, the charges $g(t)$ with the associated currents $\iota(t)$ are chosen as independent variables

$$g(t) = g(t_0) + \int_{t_0}^{t} \iota(\tau)\,\mathrm{d}\tau. \tag{15}$$

For the currents, the symbol ι is used to distinguish between derivatives $i = \mathrm{d}\iota/\mathrm{d}t$ of the currents and the currents ι themselves. The differential equations describing the dynamics of the system can be set up with a mesh analysis or the more general loop analysis [9]. Both methods balance the voltages in a loop using Kirchhoff's voltage law (KVL). In the flux approach, the fluxes $\varphi(t)$ and the voltages $u(t)$ are chosen as independent variables, where the fluxes are obtained from the voltages by integration

$$\varphi(t) = \varphi(t_0) + \int_{t_0}^{t} u(\tau)\,\mathrm{d}\tau. \tag{16}$$

In literature [8], the entity $\varphi(t)$ is sometimes also referred to as flux linkage. A node analysis, or the more general cut-set analysis, is applied, to set up the differential equations of the system. Both methods balance the currents using Kirchhoff's current law

(KCL). The duality between voltage $u(t)$ and current $\iota(t)$ of an electrical system mirror the duality in mechanics between velocity $v(t)$ and force $f(t)$. Table 1 is therefore completed with a column for the momentum approach, which is dual to the position approach in the same way as the charge approach is dual to the flux approach. The momentum $p(t)$ and the forces $f(t)$ are chosen as independent variables in the momentum approach, where the force $f(t)$ is the time-derivative of the momentum $p(t)$

$$p(t) = p(t_0) + \int_{t_0}^{t} f(\tau)\,\mathrm{d}\tau. \tag{17}$$

The differential equations are obtained from a balance of velocities in a loop. The branch relations in electronics connect the branch voltage $u(t)$ and the branch current $\iota(t)$ and correspond to the constitutive equations in mechanics connecting the velocities $v(t)$ and the forces $f(t)$. The analogy for the local variables is summarised in the first row of Table 1. The analogous elements in mechanics and electronics are given in the last three rows of Table 1. Not all electrical systems have a proper mechanical analogue, because all mass elements in mechanics measure their acceleration relative to the inertial system. The analogous electrical elements, inductivity and capacity, use branch voltages $u(t)$ and branch currents $\iota(t)$ that do not all have a common reference. For the position–flux and the momentum–charge analogy the topologies of the corresponding networks are the same in both mechanics and electronics. The corresponding networks for the position–charge and the momentum–flux analogy are dual in the sense of dual graphs. In the following sections, the electrical systems will be related to a mechanical system by using

the position approach, because most of the methods and tools in mechanics are available for this approach.

3.2 Non-smooth analogy

Since the inertia elements link one of the dual variables $f(t)$, $v(t)$ and $u(t)$, $\iota(t)$ to the derivative of the other, only the non-differentiated variable may be impulsive, in the sense of Dirac impulses, in each approach. Discontinuities are allowed for the differentiated variables, but they may not be impulsive (cf. Table 2). Actually, this is required for the local variables at the inertia element only, but in order to avoid additional difficulties, the assumption on the impulsiveness of the dual variables is extended to the complete system. Thus, the voltage $u(t)$ can be impulsive in the charge approach, while the current $\iota(t)$ is always finite. In contrast, the flux approach allows the currents $\iota(t)$ to be impulsive, while the voltage $u(t)$ is always finite. We restrict ourselves to these kinds of discontinuities. Higher order discontinuities – that may also occur in particular systems – are out of the scope of this paper. A general method of classifying such discontinuities may be found in [1]. With an impulsive branch voltage U at an inductivity, a jump in the branch current $\iota(t)$ can be forced. To change the branch voltage $u(t)$ of a capacity instantaneously,

an impulsive current I is needed (cf. Table 2). For mechanical systems, this is analogous: The force $f(t)$ may be impulsive in the position approach and must be finite in the momentum approach, whereas the velocity $v(t)$ is allowed to be impulsive only in the momentum approach and has to be finite in the position approach. If an impulsive force F is applied to a mass, then the velocity $v(t)$ of the mass changes instantaneously. In order to achieve a force jump at a spring, the position needs to jump as well, leading to an impulsive velocity V (cf. Table 2). The general non-impulsiveness of velocities in the position approach leads to continuous functions for the positions. This means that mechanical systems are not allowed to have position jumps in the position approach, which limits the applicability to real systems. If position jumps are required, then one has to use the momentum approach to allow for impulsive velocities. At the same time, the system may not contain impulsive forces anymore. The same difficulties occur in electronics due to the required continuity of the charges in the charge approach and fluxes in the flux approach. Both dual descriptions in mechanics and electronics are no longer equivalent for non-smooth dynamics as they have been for smooth dynamics.

4 Flux approach

In this section, the modelling of circuits with non-smooth switches and idealized diodes is described. The models are formulated using the flux approach and are related to their mechanical analog in the position approach. The correspondence between the local variables of the position and the flux approach is listed in Table 3. The function spaces and assumptions used for non-smooth mechanical systems in the position approach are adopted for electrical systems in the flux approach. Most of the following material has been taken from [12, 13]. The time is denoted by t and

Table 2 Impulsive variables in mechanics and electronics

Table 3 Corresponding local variables (position-flux analogy)

Mechanics	Electronics
Position $r(t)$	Flux $\varphi(t)$
Velocity $v(t)$	Voltage $u(t)$
Force $f(t)$	Current $\iota(t)$
Impulsive force $F(t)$	Impulsive current $I(t)$

the Lebesgue measure on $\mathbb{R}$ by dt. The dynamics of the system is analyzed on the compact time interval $I := [t_A, t_E]$. The velocities $v(t)$ and the branch voltages $u(t)$ are assumed to be functions of bounded variations on I, admitting an at most countable number of finite jumps. The number of discontinuity events itself does not need to be finite. The set of points at which the velocity $v(t)$ in mechanics or the voltage $u(t)$ in electronics is discontinuous, is denoted by $\{t_i\}$. For the functions $v(t)$ and $u(t)$, there exist always a left $v^-(t)$, $u^-(t)$ and a right limit $v^+(t)$, $u^+(t)$

$$v^-(t) := \lim_{\tau \uparrow 0} v(t + \tau), \quad u^-(t) := \lim_{\tau \uparrow 0} u(t + \tau),$$
$$v^+(t) := \lim_{\tau \downarrow 0} v(t + \tau), \quad u^+(t) := \lim_{\tau \downarrow 0} u(t + \tau). \tag{18}$$

The value of the velocities $v(t)$ and the branch voltages $u(t)$ is not defined for the discontinuity points $\{t_i\}$. At the points $\{t_i\}$, only the left and the right limits are defined, for which different values $v^+(t) \neq v^-(t)$, $u^+(t) \neq u^-(t)$ are obtained. For time-instances t not belonging to the set $\{t_i\}$, the left and right limits have equal values $v^+(t) = v^-(t)$, $u^+(t) = u^-(t)$. Since the functions $v(t)$ and $u(t)$ are discontinuous, they cannot be obtained by integration from their time derivatives $\dot{v}(t)$ and $\dot{u}(t)$ in the classical sense. Therefore, the derivatives $\dot{v}(t)$ and $\dot{u}(t)$ have to be understood as parts of the differential measures dv, du. The velocities $u(t)$ and branch voltages $v(t)$ are then obtained by integration of their associated differential measures dv and du

$$v^+(t) = v^-(t_A) + \int_{[t_A, t]} dv,$$
$$u^+(t) = u^-(t_A) + \int_{[t_A, t]} du. \tag{19}$$

The differential measures dv, du of the velocities $v(t)$ and voltages $u(t)$ can be split into a Lebesgue part and a purely atomic part

$$dv = \dot{v}\, dt + (v^+ - v^-)\, d\eta,$$
$$du = \dot{u}\, dt + (u^+ - u^-)\, d\eta, \tag{20}$$

corresponding to the absolutely continuous part and the step function of $v(t)$ and $u(t)$. Functions of bounded variation generally decompose into an absolutely continuous part, a step function and a singular part. In this

framework of modelling, the singular part is assumed to vanish. The measure $d\eta$ of the atomic part is concentrated on the set of discontinuity points $\{t_i\}$ of the velocities $v(t)$ and branch voltages $u(t)$. It can be written as a sum of Dirac point measures $d\delta_i$,

$$d\eta = \sum_i d\delta_i, \quad \int_A d\delta_i = \begin{cases} 1, & t_i \in A, \\ 0, & t_i \notin A, \end{cases} \tag{21}$$

where A is any one-dimensional cell in I. For smooth systems the atomic as well as the singular part of the differential measure vanish. The resulting differential measures $\dot{v}(t)\, dt$ and $\dot{u}(t)\, dt$ can be expressed completely by the time derivatives $\dot{v}(t)$ and $\dot{u}(t)$ as is done in the classical setting.

The positions $r(t)$ and the branch fluxes $\varphi(t)$ are obtained from the velocities $v(t)$ and the branch voltages $u(t)$ by integration

$$\forall t \in I: \quad r(t) = r(t_A) + \int_{t_A}^t v(\tau)\, d\tau,$$
$$\varphi(t) = \varphi(t_A) + \int_{t_A}^t u(\tau)\, d\tau, \tag{22}$$

leading to absolutely continuous functions $r(t)$ and $\varphi(t)$ on I. Note that systems which require jumps in the positions or in the fluxes cannot be modeled using the above assumptions and the position approach in mechanics or the flux approach in electronics.

4.1 Models of classical elements

The mass m in mechanics and the capacity C in electronics are the analogous inertia elements of the position–flux analogy. The resistance in electronics is related to the damping in mechanics for both the charge- and the flux-approach, but the damping coefficient d is perfectly analogous only to the inverse resistance (conductance) $1/R$ in the position–flux analogy. The analogue of the stiffness coefficient k is the inverse inductivity $1/L$. For smooth dynamics, the constitutive equations of the inertia elements

$$-m\dot{v} = f, \quad -C\dot{u} = \iota, \tag{23}$$

are formulated using the derivatives $\dot{v}(t)$, $\dot{u}(t)$, the finite forces $f(t)$ and the finite currents $\iota(t)$. With the introduction of non-smooth dynamics, allowing for jumps in

Table 4 Differential measures

$d\mathcal{F} = f \, dt + F \, d\eta$	(Force) impulsion (differential) measure
$d\mathcal{V} = v \, dt + V \, d\eta$	Velocity impulsion (differential) measure
$d\mathcal{U} = u \, dt + U \, d\eta$	Voltage impulsion (differential) measure
$d\mathcal{I} = \iota \, dt + I \, d\eta$	Current impulsion (differential) measure
$df = \dot{f} \, dt + (f^+ - f^-) \, d\eta$	Force differential measure
$dv = \dot{v} \, dt + (v^+ - v^-) \, d\eta$	Velocity differential measure
$du = \dot{u} \, dt + (u^+ - u^-) \, d\eta$	Voltage differential measure
$d\iota = i \, dt + (\iota^+ - \iota^-) \, d\eta$	Current differential measure

the velocities $v(t)$ and branch voltages $u(t)$, the derivatives $\dot{v}(t)$ and $\dot{u}(t)$ have been extended to the differential measures dv and du. A jump in the velocities $v(t)$ or the voltages $u(t)$ at the inertia element requires an impulsive force F or an impulsive current I, respectively (cf. Section 3). Therefore, the forces $f(t)$ and the currents $\iota(t)$ are replaced with differential measures by introducing force impulsion measures $d\mathcal{F}$ and current impulsion measures $d\mathcal{I}$. The measures $d\mathcal{F}$ and $d\mathcal{I}$ can be decomposed into a Lebesgue and an atomic part just as for the differential measures dv and du

$$d\mathcal{F} = f \, dt + F \, d\eta, \quad d\mathcal{I} = \iota \, dt + I \, d\eta. \qquad (24)$$

They may consist of the classical Lebesgue-measurable forces $f(t)$ and branch currents $\iota(t)$ and the purely atomic impulsive forces F and impulsive currents I. It has to be noted, that the force impulsion $\mathcal{F}$ and the current impulsion $\mathcal{I}$ are integral-entities of the force and current, respectively. This means that the current impulsion measure $d\mathcal{I}$ used in the flux approach is not equal to the current differential measure $d\iota$ used in the charge approach [13]. Table 4 gives an overview of the various differential measures and notations that are used in the four approaches in mechanics and electronics. An impact is defined as an event with a discontinuity in the velocity $v(t)$ or the voltage $u(t)$, respectively, together with non-vanishing impulsive forces F or currents I. At the inertia elements, discontinuities in the velocity $v(t)$ and the voltage $u(t)$ may only occur with an impact. The constitutive equations of the inertia elements can be extended with the differential measures dv, du, $d\mathcal{F}$ and $d\mathcal{I}$ to the non-smooth case, by writing them as equalities of measures

$$-m \, dv = d\mathcal{F}, \quad -C \, du = d\mathcal{I}. \qquad (25)$$

Since the velocity $v(t)$, position $r(t)$, voltage $u(t)$ and flux $\varphi(t)$ are always finite in the position- and the flux-
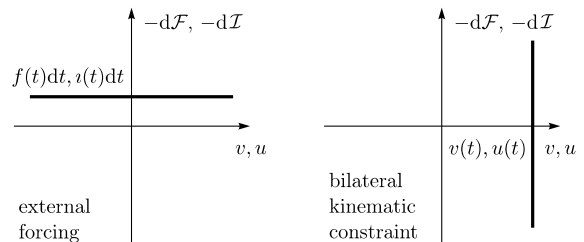

Fig. 3 Characteristics of the source elements

approach, only finite forces $f(t)$ and currents $\iota(t)$ are required at damping, resistance, stiffness and inductivity elements. Discontinuities in the velocity $v(t)$ and the voltage $u(t)$ can occur for these elements without impact. The constitutive equations remain the same for these elements as in the case of smooth dynamics. Table 5 summarizes the position–flux analogy for the classical elements. In electronics, usually the voltage source and the current source are introduced as elements as well. A voltage source defines the branch voltage $u(t)$ as an explicit function of time, leaving the branch current $\iota(t)$ unconstrained. The corresponding mechanical element in the position–flux analogy is the bilateral kinematic constraint (or prescribed velocity). In contrast, the branch current $\iota(t)$ is defined as a function of time for the current source. The analogous mechanical element is the external force (cf. Table 6). For the position- and flux-approach respectively, the voltage source and the bilateral kinematic constraint are set-valued elements, while the current source and the external force are single valued elements (cf. Fig. 3).

4.2 Models of non-smooth elements

The switching elements are modeled as ideal non-smooth circuit components. By idealizing the elements, the numerical problems of stiff differential equations are avoided. As in mechanics, set valued branch relations are introduced to characterise the behaviour of
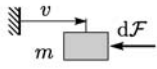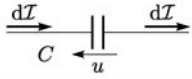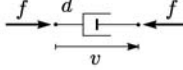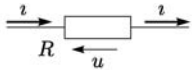
Table 5 Classical elements

	mechanics	electronics
inertia	m mass $-m\,dv = d\mathcal{F}$	C capacity $-C\,du = d\mathcal{I}$
dissipation	d damping coefficient $-dv = f$	R resistance $-\frac{1}{R}u = \imath$
energy storage	k stiffness coefficient $-kr = f$	L inductivity $-\frac{1}{L}\varphi = \imath$
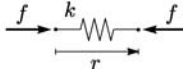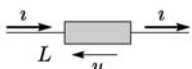
Table 6 Source elements

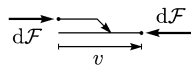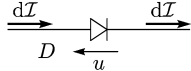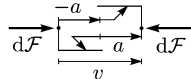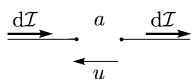|	mechanics	electronics
external forcing	f force $f = f(t),\ v \in \mathbb{R}$	$\imath$ current source $\imath = \imath(t),\ u \in \mathbb{R}$
bilateral kinematic constraint	v velocity $-d\mathcal{F} \in \mathbb{R},\ v = v(t)$	u voltage source $-d\mathcal{I} \in \mathbb{R},\ u = u(t)$
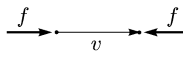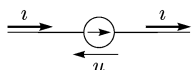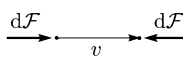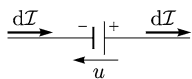
the elements. This leads to measure differential inclusions as description of the dynamics of the system. For the existence and uniqueness of the solution of the system of measure differential inclusions, the maximality and monotonicity of the set-valued maps used for the branch relations are important properties. The most basic non-smooth and set-valued elements that occur in electronics and their mechanical analog are shown in Table 7. The unilateral kinematic constraint element is a sprag clutch in mechanics and a diode in electronics. The sprag clutch limits the relative velocity to nonnegative values, by allowing unbounded positive forces for zero relative velocity. If the velocity of the sprag clutch is positive, then the force is zero. The current through an ideal diode may flow only in the positive direction. To prevent the current from flowing in the negative direc-

tion, an ideal diode can provide an unbounded voltage at zero current. Both characteristics can be expressed with the set-valued relations

$$-f \in \mathrm{Upr}(v), \quad -\imath \in \mathrm{Upr}(u), \quad t \notin \{t_i\}, \tag{26}$$

using the unilateral primitive Upr. The sprag clutch and the diode cannot produce impacts by themselves during the evolution of the dynamics, but they may carry unbounded forces and currents, allowing them to react on impacts. Additionally, they may produce an impact at the beginning of the motion, if the system is initialised with non-feasible velocities or voltages. Therefore, the constitutive laws (26) have to be completed with impact laws

Table 7 Non-smooth elements

	mechanics	electronics
unilateral kinematic constraint	sprag clutch $-\mathrm{d}\mathcal{F} \in \mathrm{Upr}(v^+)$	diode $-\mathrm{d}\mathcal{I} \in \mathrm{Upr}(u^+)$
parallel unilateral kinematic constraint	parallel sprag clutch $-\mathrm{d}\mathcal{F} \in$ $\mathrm{Upr}(a^+ + v^+) - \mathrm{Upr}(a^+ - v^+)$	spark gap / switch $-\mathrm{d}\mathcal{I} \in$ $\mathrm{Upr}(a^+ + u^+) - \mathrm{Upr}(a^+ - u^+)$
shifted unilateral kinematic constraint	moving sprag clutch $-\mathrm{d}\mathcal{F} \in \mathrm{Upr}(a^+ + v^+)$	unilateral switch $-\mathrm{d}\mathcal{I} \in \mathrm{Upr}(a^+ + u^+)$
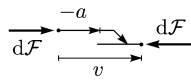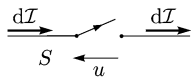
$$-F \in \mathrm{Upr}(v^+), \quad -I \in \mathrm{Upr}(u^+), \quad t \in \{t_i\}, \qquad (27)$$

allowing for a completely inelastic impact behaviour. The constitutive laws (26) for the continuous part of the motion and the impact laws (27) for the discontinuity events can be expressed with a single measure inclusion

$$-\mathrm{d}\mathcal{F} \in \mathrm{Upr}(v^+), \quad -\mathrm{d}\mathcal{I} \in \mathrm{Upr}(u^+). \qquad (28)$$

To show that the measure inclusion (28) contains both laws (26) and (27), the decomposition (24) for the current impulsion measures is put into Equation (28). The resulting expression

$$-\iota\,\mathrm{d}t - I\,\mathrm{d}\eta \in \mathrm{Upr}(u^+) \qquad (29)$$

can now be simplified for times $t \in \{t_i\}$ at which discontinuity events take place and times $t \notin \{t_i\}$ where the voltage $u(t)$ is continuous. For times $t \notin \{t_i\}$, the atomic part $\mathrm{d}\eta$ is zero, whereas for the set of discontinuities $\{t_i\}$ the Lebesgue measure $\mathrm{d}t$ can be neglected in the sense of integration. For the two cases one obtains

$$\begin{cases} -\iota\,\mathrm{d}t \in \mathrm{Upr}(u^+), & t \notin \{t_i\}, \\ -I\,\mathrm{d}\eta \in \mathrm{Upr}(u^+), & t \in \{t_i\}. \end{cases} \qquad (30)$$

Since the measures $\mathrm{d}t$ and $\mathrm{d}\eta$ are strictly positive, they can be eliminated with the help of the unilateral primi-
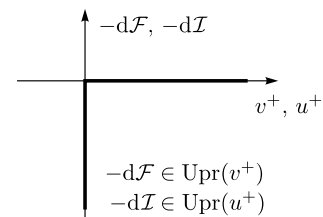
Fig. 4 Characteristic of sprag clutches and diodes

tive Upr. For the continuous parts $t \notin \{t_i\}$ of the motion, the right limit u^+ is always equal to u. Finally, one obtains the relations

$$\begin{cases} -\iota \in \mathrm{Upr}(u), & t \notin \{t_i\}, \\ -I \in \mathrm{Upr}(u^+), & t \in \{t_i\}, \end{cases} \qquad (31)$$

which are the same as in Equations (26) and (27). The characteristic of the sprag clutch and the diode is depicted in Fig. 4. It has to be noted that, due to the different assumptions on the continuity of the charge $g(t)$ and the flux $\varphi(t)$ in the two electrical approaches, the resulting model for the ideal diode is different as well. In contrast to the flux approach, the charge approach allows an impulsive voltage U and a finite current $\iota(t)$ at a diode, leading to the model

$$-\mathrm{d}\mathcal{U} \in \mathrm{Upr}(\iota^+). \qquad (32)$$

The second element in Table 7 is the ideal spark gap with variable break-through voltage, which is a good model for switches at the same time [13]. Using the charge approach, the impact-free dynamics of a spark gap can be described with the relation

$$-u \in a \cdot \mathrm{Sgn}(\iota), \quad t \notin \{t_i\}, \tag{33}$$

where $a > 0$ is the break-through voltage. If the current flowing across the spark gap is zero, then the voltage can vary between $-a$ and a. The branch voltage u can never exceed the voltage boundaries $-a$ and a. To enforce this, the element can supply any positive current ι at the voltage $u = -a$ to prevent the voltage from falling further. In a symmetric way, the element allows any negative branch current ι at the voltage $u = a$. For the flux approach, the inclusion (33) has to be solved for the branch current ι using relation (12). The characteristic

$$-\iota \in \mathrm{Upr}(a + u) - \mathrm{Upr}(a - u), \quad t \notin \{t_i\} \tag{34}$$

is obtained for the impact-free dynamics of a spark gap in the flux approach. The branch relation of the spark gap is illustrated in Fig. 5. A switch can be seen as a spark gap with a variable gap length. For the model of the spark gap, this means that the break-through voltage a is a function of time. A break-through voltage $a = 0$ results in a perfect conductor, while an ideal isolator is obtained for $a \to \infty$. If the break-through voltage a is made to be an explicit function of time with a priori known switching times, then the model represents an externally controlled switch. An internally controlled switch is obtained by extending the dependency of the break-through voltage a to the state of the circuit. Impacts may occur, if the spark gap is initialised with non-feasible voltages or it is operated as a switch

in combination with a capacitor. The switching may produce a non-feasible initial condition for the motion starting after the switching event, requiring an impact to reestablish consistent conditions. The spark gap is equipped with the impact law

$$-I \in \mathrm{Upr}(a^+ + u^+) - \mathrm{Upr}(a^+ - u^+), \quad t \in \{t_i\} \tag{35}$$

in analogy to the impact law used for the unilateral kinematic constraint. Again, the constitutive law (34) for the continuous part of the motion and the impact law (35) for the discontinuity events can be expressed with a single measure inclusion

$$-\mathrm{d}\mathcal{I} \in \mathrm{Upr}(a^+ + u^+) - \mathrm{Upr}(a^+ - u^+). \tag{36}$$

The analogous element in mechanics consists of two parallel sprag clutches that are moved with a relative velocity a (cf. Table 7). The complete characteristic of the parallel sprag clutches and the spark gap is shown in Fig. 6. The unilateral switch has the perfect isolator and the idealized diode as the two limiting states. The model for a unilateral switch can be obtained from the bi-directional switch by taking only one Upr into account. The resulting branch relation, expressed as a differential measure inclusion,

$$-\mathrm{d}\mathcal{I} \in \mathrm{Upr}(a^+ + u^+) \tag{37}$$

Fig. 5 Branch relation of spark gaps

Fig. 6 Characteristic of parallel sprag clutches and spark gaps

Fig. 7 Characteristic of moving sprag clutches and unilateral switches

is depicted in Fig. 7. In mechanics, the unilateral switch corresponds to a single sprag clutch that is moved with the velocity a (cf. Table 7).
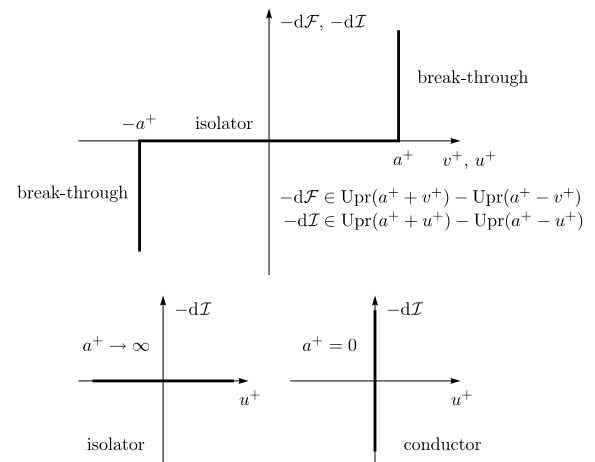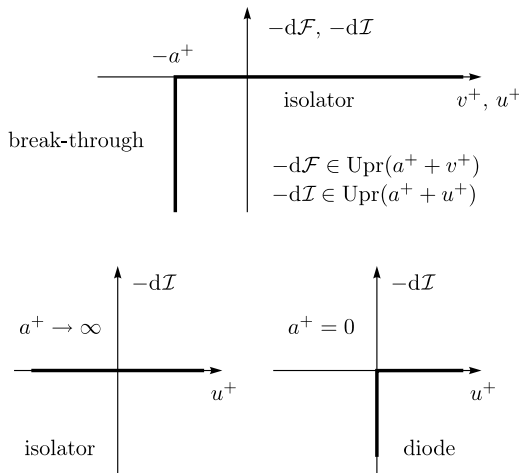
4.3 Kirchhoff's laws

The differential equations, describing the dynamics of a mechanical system, are usually derived using the principle of virtual work. The virtual work of a mechanical system

$$\delta W := \int_S \delta \boldsymbol{\xi}^{\mathrm{T}} (\ddot{\boldsymbol{\xi}} \, \mathrm{d}m - \mathrm{d}\boldsymbol{F}) \tag{38}$$

is formed with the virtual displacements $\delta\boldsymbol{\xi}$, the inertia force density $\ddot{\boldsymbol{\xi}} \, \mathrm{d}m$ and the force density $\mathrm{d}\boldsymbol{F}$, containing both internal and external forces. If the constraint forces are considered in the virtual work as well, then the principle of virtual work can be formulated as

$$\delta W = 0 \ \forall \, \delta\boldsymbol{\xi} \ \Rightarrow \ \begin{array}{l} \text{mechanical system is in} \\ \text{dynamic equilibrium.} \end{array} \tag{39}$$

The integral in the definition of the virtual work (38) can be replaced by a sum for lumped parameter systems. The expression $\ddot{\boldsymbol{\xi}} \, \mathrm{d}m$ can be interpreted as inertia forces on the mass elements, leading to a virtual work expression that is formed only by products of forces and virtual displacements. With the introduction of force impulse measures $\mathrm{d}\mathcal{F}$, the virtual action $\mathrm{d}\delta W$ is used

instead of the virtual work δW. This leads to the definition

$$\mathrm{d}\delta W := \sum_i \mathrm{d}\mathcal{F}_i \delta r_i \tag{40}$$

for the virtual action of a mechanical lumped parameter system. The sum is taken over all elements of the system, while $\mathrm{d}\mathcal{F}_i$ denotes the force impulse measure and δr_i the virtual displacement at the ith element. The definition of the virtual action of an electrical lumped parameter system

$$\mathrm{d}\delta W := \sum_i \mathrm{d}\mathcal{I}_i \delta \varphi_i \tag{41}$$

is obtained using the position–flux analogy. The virtual action at the ith element is formed with the branch current impulse measure $\mathrm{d}\mathcal{I}_i$ and the virtual flux displacement $\delta\varphi_i$. The principle of d'Alembert/Lagrange states that constraint forces of perfect constraints, which do not produce any virtual work for admissible virtual displacements, can be omitted in the virtual work expression, if the variation considers only admissible virtual displacements. Correspondingly, the principle (39) can be reformulated as

$$\mathrm{d}\delta W = 0 \ \forall \, \delta r_i^{\mathrm{adm}} \ \Rightarrow \ \begin{array}{l} \text{mechanical system is in} \\ \text{dynamic equilibrium} \\ \text{w.r.t. free directions} \end{array} \tag{42}$$

for mechanical systems, where $\delta r_i^{\mathrm{adm}}$ denotes any virtual displacements that are compatible with the constraints. In the virtual action, the constraint force impulsion measures of the perfect constraints have no longer to be considered. For electrical systems, the principle

$$\mathrm{d}\delta W = 0 \ \forall \, \delta \varphi_i^{\mathrm{adm}} \ \Rightarrow \ \begin{array}{l} \text{electrical system is in} \\ \text{dynamic equilibrium} \\ \text{w.r.t. free directions} \end{array} \tag{43}$$

is formulated analogously. The admissible virtual flux displacements are denoted by $\delta\varphi_i^{\mathrm{adm}}$. Due to the constraints introduced by the connections in an electrical circuit, not all $\delta\varphi_i$ are admissible. To be able to give a formulation for the admissible virtual flux displacements $\delta\varphi_i^{\mathrm{adm}}$, the kinematics of a circuit is analysed first. In Fig. 8, the connection of independent electrical elements in a circuit is illustrated. A formulation of the
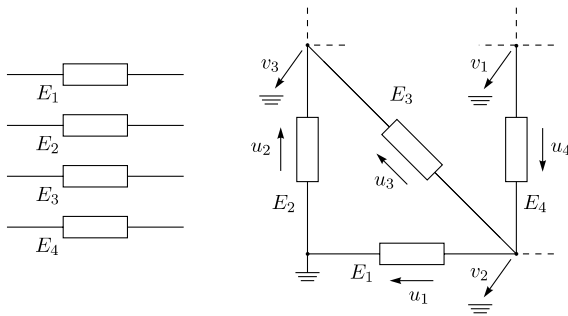
Fig. 8 Electrical elements connected into a circuit

constraints imposed on the system can be obtained by applying Kirchhoff's voltage law (KVL). The branch voltages $u(t)$ and branch fluxes $\varphi(t)$ of a circuit are no longer independent, and a description using a reduced set of variables may be obtained. A voltage is defined only with respect to a reference point, in analogy to the velocity in mechanics. An arbitrary node is therefore selected as the reference node, and the voltages $v_i(t)$ of all other nodes are defined with respect to this reference. The ground node is usually taken as the reference node. The nodal voltages v_i and the nodal fluxes q_i form the reduced set of variables. The nodal voltages v_i may be collected into a vector of nodal voltages or generalised voltages

$$
\boldsymbol{v} := \begin{pmatrix} v_1 \\ v_2 \\ \vdots \\ v_{n-1} \end{pmatrix}, \quad \boldsymbol{q} := \begin{pmatrix} q_1 \\ q_2 \\ \vdots \\ q_{n-1} \end{pmatrix}, \tag{44}
$$

with an associated vector of nodal fluxes or generalized coordinates $\boldsymbol{q}$. As for the branch flux $\varphi(t)$ and the branch voltage $u(t)$, it holds that the nodal voltages $\boldsymbol{v}$ are the time derivatives of the nodal fluxes $\boldsymbol{q}$ dt-almost everywhere, i.e.

$$
\dot{\boldsymbol{q}} = \boldsymbol{v}, \quad \mathrm{d}t\text{-almost everywhere.} \tag{45}
$$

Within the position–flux analogy, nodal fluxes and voltages correspond to generalized coordinates and velocities, respectively. It has to be noted that the generalized coordinates used in mechanics are usually minimal coordinates with respect to the bilateral kinematic constraints. In contrast, the voltage source element is not considered here in the process of defining the generalised coordinates for electrical circuits, leading to a

differential algebraic system (DAE) as description. All branch voltages satisfying Kirchhoff's voltage law can be expressed by the nodal voltages $\boldsymbol{v}$,

$$
u_i = \boldsymbol{w}_i^{\mathrm{T}} \boldsymbol{v}, \tag{46}
$$

as a branch voltage is equal to the difference between the two voltages at the nodes it connects. Equation (46) is called the nodal transformation [18], and defines the node-branch incidence matrix. The nodal transformation (46) holds also in integrated form

$$
\varphi_i = \boldsymbol{w}_i^{\mathrm{T}} \boldsymbol{q}, \tag{47}
$$

relating the nodal fluxes $\boldsymbol{q}$ to the branch fluxes φ_i. There is no nodal voltage $\boldsymbol{v}$ that could violate the constraints described by the KVL equations, and all possible branch voltages u_i can be expressed using $\boldsymbol{v}$. Therefore, the admissible virtual flux displacements $\delta\varphi_i^{\mathrm{adm}}$ can be obtained by transforming arbitrary virtual nodal flux displacements $\delta\boldsymbol{q}$ with the nodal transformation (46)

$$
\delta\varphi_i^{\mathrm{adm}} = \boldsymbol{w}_i^{\mathrm{T}} \delta\boldsymbol{q}. \tag{48}
$$

With this relation the formulation (43) may be further simplified

$$
0 = \mathrm{d}\delta W = \sum_i \mathrm{d}\mathcal{I}_i \boldsymbol{w}_i^{\mathrm{T}} \delta\boldsymbol{q} = \delta\boldsymbol{q}^{\mathrm{T}} \sum_i \boldsymbol{w}_i \, \mathrm{d}\mathcal{I}_i \ \ \forall \, \delta\boldsymbol{q}. \tag{49}
$$

Since this variational equation is formulated for arbitrary $\delta\boldsymbol{q}$, it can be reduced to the equation

$$
\sum_i \boldsymbol{w}_i \, \mathrm{d}\mathcal{I}_i = 0, \tag{50}
$$

which is identified as Kirchhoff's current law. Associated with the nodes of a circuit, a generalised current impulsion measure $\mathrm{d}\mathcal{J}$ can be defined

$$
\mathrm{d}\mathcal{J} := \sum_i \boldsymbol{w}_i \, \mathrm{d}\mathcal{I}_i. \tag{51}
$$

Each component of the generalized current impulsion measure $\mathrm{d}\mathcal{J}$ is the sum of all current impulsion measures flowing into or out of the corresponding node.

Fig. 9 The DC–DC buck converter
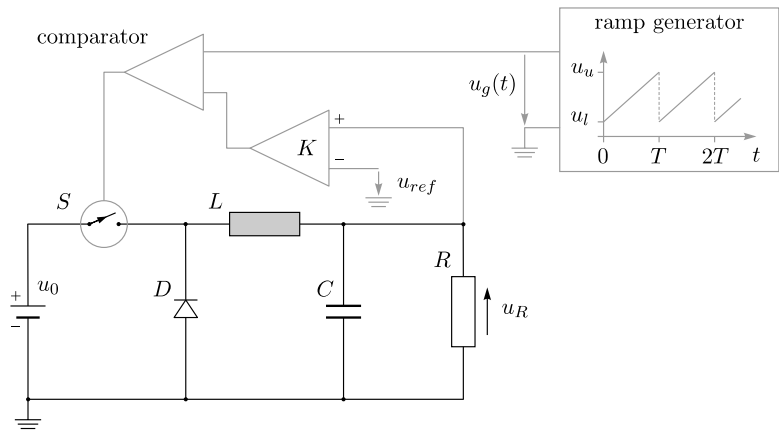
Kirchhoff's current law for non-smooth systems (50) can be reduced to

$$\mathrm{d}\mathcal{J} = 0 \tag{52}$$

using definition (51).

5 DC–DC buck converter

In this section, the theory and methods that have been presented in the previous sections are applied to an example, being the DC–DC buck converter. The electrical model is formulated in the flux approach and related to an analogous mechanical model using the position–flux analogy. The model and notation are kept as similar as possible to the one used in [13], to allow for an easy comparison of the two approaches. A general DC–DC converter is a circuit that allows for the efficient conversion of DC electrical power from one voltage level to another. For the DC–DC buck converter, the voltage at the output is smaller than the voltage at the input of the circuit. The circuit of a controlled DC–DC buck converter is shown in Fig. 9. Besides the classical elements R, C, L and the voltage source u_0, the circuit consists of an ideal diode D and a unilateral switch S. The voltage u_0 supplied by the voltage source is converted to a lower voltage u_R at the resistive load R. The part of Fig. 9, which is drawn in grey, shows the switch control of the DC–DC buck converter, which controls the voltage at the load R by operating the unidirectional switch S. There occur no impacts (discontinuities in the voltages, together with non-vanishing impulsive currents) during the evolution of the dynamics of the circuit, if non-feasible initial conditions are excluded.

However, due to the operation of the switch, there are discontinuity events in the dynamics of the DC–DC buck converter, but they do not lead to impacts.

5.1 The switch control of the DC–DC buck converter

In this section, a model of the switch control is described. The switch control of the DC–DC buck converter consists of an amplifier with gain K, a comparator and a ramp generator with period T, lower voltage u_l and upper voltage u_u (cf. Fig. 10). The output voltage a of the switch control is used to operate the unilateral switch S of the buck converter. With the output voltage u_{comp} of the amplifier

$$u_{\mathrm{comp}} = -K(u_R + u_{\mathrm{ref}}) \tag{53}$$

and the explicitly time-dependent output voltage $u_g(t)$ of the ramp generator

$$u_g(t) = u_l + \left(\frac{t}{T} - k\right)(u_u - u_l)$$

$$kT \leq t < (k+1)T; \quad k = 0, 1, 2, \ldots \tag{54}$$
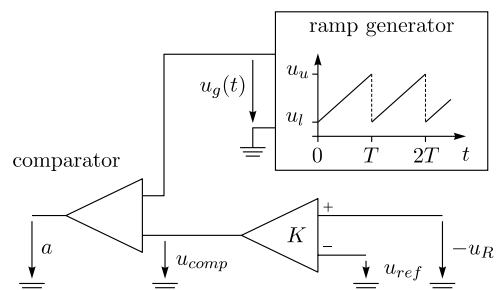

Fig. 10 Model of the switch control

the voltage a at the comparator can be written as

$$a = \begin{cases} 0, & u_{\text{comp}} - u_g(t) \leq 0, \\ +\infty, & u_{\text{comp}} - u_g(t) > 0. \end{cases} \quad (55)$$

This relation can be simplified by eliminating u_{comp} and defining

$$h(t) := u_{\text{ref}} + \frac{1}{K} u_g(t) \quad (56)$$

resulting in the following rule for the switch control

$$a(u_R, t) = \begin{cases} 0, & -u_R(t) \leq h(t), \\ +\infty, & -u_R(t) > h(t). \end{cases} \quad (57)$$

For $a = 0$, the switch is closed and behaves as an ideal diode, while the switch is perfectly isolating for $a = +\infty$.

5.2 The extended DC–DC buck converter

In this section, the measure differential inclusions for an extended model of the DC–DC buck converter are derived. The extended DC–DC buck converter has two additional capacitors C^* and C° compared to the original DC–DC buck converter, in order to assure a non-singular matrix M of capacitances. This extension of the circuit is done to arrive at a system that complies with Lagrangian dynamics and which eases the analogy to mechanical systems, for which positive definiteness and symmetry of the associated matrix of inertias M is always presupposed. The circuit of the original DC–DC buck converter is obtained by setting the two additional

capacities C^* and C° to zero. The circuit of the extended DC–DC buck converter as shown in Fig. 11 has four nodes. To emphasise the four nodes of the circuit, they have been shaded grey in Fig. 11. The ground node is chosen as reference, while the nodal voltages v_1, v_2 and v_3 are introduced for the three remaining nodes. Every nodal voltage v_i has an associated nodal flux q_i. The nodal voltages v_i are sometimes called generalized voltages as well, while the nodal fluxes q_i are referred to as generalized coordinates. The vector of nodal voltages v and the associated vector of nodal fluxes q as defined in Equation (44) become

$$q := \begin{pmatrix} q_1 \\ q_2 \\ q_3 \end{pmatrix}, \quad v := \begin{pmatrix} v_1 \\ v_2 \\ v_3 \end{pmatrix},$$

$$\dot{q} = v \ \mathrm{d}t\text{-almost everywhere}, \quad (58)$$

for the extended DC–DC buck converter. With the definition of the nodal voltages, the branch voltages u_i may be written as a linear combination of the form (46), defining the nodal transformation of the circuit. From the nodal transformation

$$\begin{aligned} u_0 &= w_0^{\mathrm{T}} v = v_1 & \Rightarrow w_0^{\mathrm{T}} &= (1, 0, 0) \\ u_{C^*} &= w_{C^*}^{\mathrm{T}} v = v_1 & \Rightarrow w_{C^*}^{\mathrm{T}} &= (1, 0, 0) \\ u_S &= w_S^{\mathrm{T}} v = v_2 - v_1 & \Rightarrow w_S^{\mathrm{T}} &= (-1, 1, 0) \\ u_D &= w_D^{\mathrm{T}} v = v_2 & \Rightarrow w_D^{\mathrm{T}} &= (0, 1, 0) \\ u_C &= w_C^{\mathrm{T}} v = -v_3 & \Rightarrow w_C^{\mathrm{T}} &= (0, 0, -1) \\ u_L &= w_L^{\mathrm{T}} v = v_3 - v_2 & \Rightarrow w_L^{\mathrm{T}} &= (0, -1, 1) \\ u_{C^\circ} &= w_{C^\circ}^{\mathrm{T}} v = v_2 & \Rightarrow w_{C^\circ}^{\mathrm{T}} &= (0, 1, 0) \\ u_R &= w_R^{\mathrm{T}} v = -v_3 & \Rightarrow w_R^{\mathrm{T}} &= (0, 0, -1) \end{aligned} \quad (59)$$

Fig. 11 Electrical model of the extended DC–DC buck converter
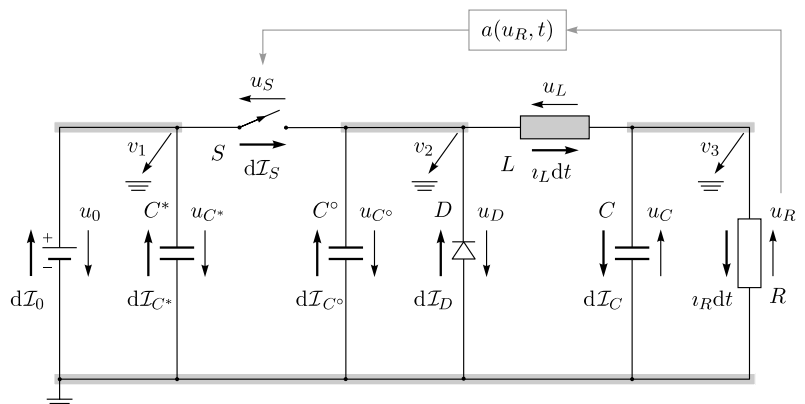
the vectors $\boldsymbol{w}_i$ required for the virtual action $\mathrm{d}\delta W$ can be obtained directly. Kirchhoff's current law

$$0 = \mathrm{d}\mathcal{J} = \sum_i \boldsymbol{w}_i \, \mathrm{d}\mathcal{I}_i, \tag{60}$$

which has been related to the virtual action of electrical systems in Section 4.3, may now be evaluated with the help of the nodal transformation (59), yielding

$$
\begin{aligned}
\mathrm{d}\mathcal{J}_1 &= \mathrm{d}\mathcal{I}_0 + \mathrm{d}\mathcal{I}_{C^*} - \mathrm{d}\mathcal{I}_S = 0, \\
\mathrm{d}\mathcal{J}_2 &= \mathrm{d}\mathcal{I}_S + \mathrm{d}\mathcal{I}_D - \iota_L \, \mathrm{d}t + \mathrm{d}\mathcal{I}_{C^\circ} = 0, \\
\mathrm{d}\mathcal{J}_3 &= -\mathrm{d}\mathcal{I}_C + \iota_L \, \mathrm{d}t - \iota_R \, \mathrm{d}t = 0.
\end{aligned} \tag{61}
$$

The single-valued branch relations of the capacitors, the resistor and the inductor

$$
\begin{aligned}
\mathrm{d}\mathcal{I}_{C^*} &= -C^* \, \mathrm{d}u_{C^*}, \\
\mathrm{d}\mathcal{I}_C &= -C \, \mathrm{d}u_C, \\
\mathrm{d}\mathcal{I}_{C^\circ} &= -C^\circ \, \mathrm{d}u_{C^\circ}, \\
\iota_R \, \mathrm{d}t &= -\tfrac{1}{R} u_R \, \mathrm{d}t, \\
\iota_L \, \mathrm{d}t &= -\tfrac{1}{L} \varphi_L \, \mathrm{d}t,
\end{aligned} \tag{62}
$$

are formulated according to Table 5. After inserting the single-valued branch relations (62) into the Equations (61), and expressing the branch voltages u_i and branch fluxes φ_i by the nodal voltages v_i and nodal fluxes q_i using the nodal transformation (59), one obtains the equations

$$
\begin{aligned}
&C^* \, \mathrm{d}v_1 + \mathrm{d}\mathcal{I}_S - \mathrm{d}\mathcal{I}_0 = 0, \\
&C^\circ \, \mathrm{d}v_2 - \frac{1}{L}(q_3 - q_2) \, \mathrm{d}t - \mathrm{d}\mathcal{I}_S - \mathrm{d}\mathcal{I}_D = 0, \\
&C \, \mathrm{d}v_3 + \frac{1}{L}(q_3 - q_2) \, \mathrm{d}t + \frac{1}{R} v_3 \, \mathrm{d}t = 0.
\end{aligned} \tag{63}
$$

The branch relations of the diode, the switch and the voltage source

$$
\begin{aligned}
-\mathrm{d}\mathcal{I}_D &\in \mathrm{Upr}(u_D^+), \\
-\mathrm{d}\mathcal{I}_S &\in \mathrm{Upr}(a^+ + u_S^+), \\
-\mathrm{d}\mathcal{I}_0 &\in \mathbb{R}, \quad u_0 = u_0(t),
\end{aligned} \tag{64}
$$

are set-valued and are formulated according to Tables 6 and 7. The branch voltage u_R in the switch control of the DC–DC buck converter (57) can be replaced with

the nodal voltages, yielding

$$a(v_3, t) = \begin{cases} 0, & v_3(t) \le h(t), \\ +\infty, & v_3(t) > h(t). \end{cases} \tag{65}$$

With the switch control (65), the Equations (63) and the set-valued inclusions (64) the description of the extended DC–DC buck converter is complete. With the definition of the matrices

$$
\begin{aligned}
\boldsymbol{M} &:= \boldsymbol{w}_{C^*} \boldsymbol{w}_{C^*}^{\mathrm{T}} C^* + \boldsymbol{w}_{C^\circ} \boldsymbol{w}_{C^\circ}^{\mathrm{T}} C^\circ + \boldsymbol{w}_C \boldsymbol{w}_C^{\mathrm{T}} C, \\
\boldsymbol{D} &:= \boldsymbol{w}_R \boldsymbol{w}_R^{\mathrm{T}} \frac{1}{R}, \\
\boldsymbol{K} &:= \boldsymbol{w}_L \boldsymbol{w}_L^{\mathrm{T}} \frac{1}{L},
\end{aligned} \tag{66}
$$

the relations (63) and (64) can be written in matrix form, yielding

$$
\begin{aligned}
&\boldsymbol{M} \, \mathrm{d}\boldsymbol{v} + \boldsymbol{D} \boldsymbol{v} \, \mathrm{d}t + \boldsymbol{K} \boldsymbol{q} \, \mathrm{d}t - \boldsymbol{w}_D \, \mathrm{d}\mathcal{I}_D \\
&\quad - \boldsymbol{w}_S \, \mathrm{d}\mathcal{I}_S - \boldsymbol{w}_0 \, \mathrm{d}\mathcal{I}_0 = \boldsymbol{0}, \quad \dot{\boldsymbol{q}} = \boldsymbol{v} \ \mathrm{d}t\text{-a.e.} \\
&u_D = \boldsymbol{w}_D^{\mathrm{T}} \boldsymbol{v}, \quad -\mathrm{d}\mathcal{I}_D \in \mathrm{Upr}(u_D^+), \\
&u_S = \boldsymbol{w}_S^{\mathrm{T}} \boldsymbol{v}, \quad -\mathrm{d}\mathcal{I}_S \in \mathrm{Upr}(a^+ + u_S^+), \\
&u_0 = \boldsymbol{w}_0^{\mathrm{T}} \boldsymbol{v}, \quad -\mathrm{d}\mathcal{I}_0 \in \mathbb{R}, \quad u_0 = u_0(t),
\end{aligned} \tag{67}
$$

with

$$
\boldsymbol{M} = \begin{pmatrix} C^* & 0 & 0 \\ 0 & C^\circ & 0 \\ 0 & 0 & C \end{pmatrix}, \quad
\boldsymbol{D} = \begin{pmatrix} 0 & 0 & 0 \\ 0 & 0 & 0 \\ 0 & 0 & \frac{1}{R} \end{pmatrix},
$$

$$
\boldsymbol{K} = \begin{pmatrix} 0 & 0 & 0 \\ 0 & \frac{1}{L} & \frac{-1}{L} \\ 0 & \frac{-1}{L} & \frac{1}{L} \end{pmatrix}, \quad
\boldsymbol{w}_D = \begin{pmatrix} 0 \\ 1 \\ 0 \end{pmatrix}, \tag{68}
$$

$$
\boldsymbol{w}_S = \begin{pmatrix} -1 \\ 1 \\ 0 \end{pmatrix}, \quad
\boldsymbol{w}_0 = \begin{pmatrix} 1 \\ 0 \\ 0 \end{pmatrix},
$$

$$
\boldsymbol{q} = \begin{pmatrix} q_1 \\ q_2 \\ q_3 \end{pmatrix}, \quad
\boldsymbol{v} = \begin{pmatrix} v_1 \\ v_2 \\ v_3 \end{pmatrix}.
$$

The mechanical model associated with the extended DC–DC buck converter can be obtained from Equations (67) and (68) using the position–flux analogy. The mechanical model is illustrated in Fig. 12. The model
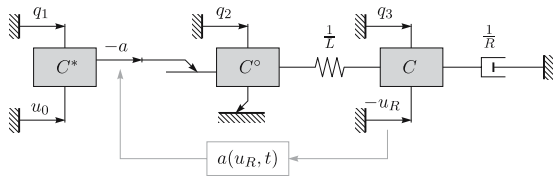
Fig. 12 Mechanical model associated with the extended DC–DC buck converter

consists of three masses C^*, C° and C corresponding to the three capacitors of the extended DC–DC buck converter. Since the position–flux analogy is used, the electrical circuit and the mechanical model have the same topology. The mass C is connected to the environment by a linear damper with damping coefficient $1/R$. A linear spring with stiffness coefficient $1/L$ connects the masses C° and C, representing the inductor of the electrical circuit. The sprag clutch acting between the environment and the mass C° is analogous to the diode and allows the mass C° to only move to the right. The masses C^* and C° are interacting by the serial connection of a kinematic excitation with relative velocity $-a$ and a sprag clutch, constituting the analogue to the unilateral switch. The velocity of the mass C^* is prescribed to be u_0. The switch control of the DC–DC buck converter measures the velocity u_R and provides the relative velocity $-a$. To solve the measure differential inclusion (67) describing the non-smooth dynamics of the circuit for the unknown nodal voltages $\boldsymbol{v}(t)$ and the associated nodal fluxes $\boldsymbol{q}(t)$, a time-stepping method is used. Time-stepping methods discretise directly the inclusion (67) over a time-step Δt. The problem of solving the measure differential inclusion (67) numerically is formulated as follows: For the system (67), with given initial nodal charges $\boldsymbol{q}_A$ and initial nodal voltages $\boldsymbol{v}_A$,

$$\boldsymbol{q}_A := \boldsymbol{q}(t_A), \quad \boldsymbol{v}_A := \boldsymbol{v}(t_A), \tag{69}$$

at the initial time t_A, find nodal charges $\boldsymbol{q}_E$ and nodal voltages $\boldsymbol{v}_E$,

$$\boldsymbol{q}_E := \boldsymbol{q}(t_E), \quad \boldsymbol{v}_E := \boldsymbol{v}(t_E), \tag{70}$$

at the time t_E which approximate the exact solution. The time t_E is the end of a chosen time interval $[t_A, t_E]$ with length

$$\Delta t := t_E - t_A. \tag{71}$$

The resulting algorithms are very robust and easy to implement, but have a limited accuracy, see e.g. [3, 14, 19] for some versions of time stepping algorithms.

The discretised differential inclusion can either be transformed into a linear complementarity problem or a set of nonlinear equations using the Augmented Lagrangian approach [2]. The formulation as a linear complementarity problem is limited to linear systems, but it can be solved with robust numerical algorithms. With the Augmented Lagrangian approach it is difficult to obtain guaranteed convergence for the numerical solution of the set of nonlinear equations. For the extended DC–DC buck converter, the transformation into a linear complementarity problem will be used. In the flux approach, the buck converter contains both smooth and non-smooth set-valued elements. The only smooth set-valued element in the buck converter is the voltage source u_0. One possibility to treat the voltage source, is to remove the state v_1 from the system by replacing v_1 with u_0, obtaining a set of minimal coordinates with respect to the bilateral constraints. For this circuit, the transformation to minimal coordinates is straightforward, because the voltage source is connected directly to the reference node with one port. As an alternative to the reduction to minimal coordinates, the branch relation of the voltage source can be expressed with two complementarity conditions and can be included into the linear complementarity problem. This means that the bilateral constraint is treated as two unilateral constraints, which is not very efficient from the numerical point of view. A third possibility is to append the current of the voltage source branch to the vector of unknown voltages after discretisation. This approach, also known in electronics as modified nodal analysis, is used in the following for the extended DC–DC buck converter. In order to simplify the expressions, the notations

$$\mathrm{d}\boldsymbol{\mathcal{I}} := \begin{pmatrix} \mathrm{d}\mathcal{I}_D \\ \mathrm{d}\mathcal{I}_S \end{pmatrix}, \quad \boldsymbol{W} := (\boldsymbol{w}_D \ \boldsymbol{w}_S) \tag{72}$$

are introduced. Using these notations the equality of measures in Equation (67) may be written as

$$\boldsymbol{M}\,\mathrm{d}\boldsymbol{v} + \boldsymbol{D}\boldsymbol{v}\,\mathrm{d}t + \boldsymbol{K}\boldsymbol{q}\,\mathrm{d}t - \boldsymbol{W}\,\mathrm{d}\boldsymbol{\mathcal{I}} - \boldsymbol{w}_0\,\mathrm{d}\mathcal{I}_0 = \boldsymbol{0},$$
$$\boldsymbol{w}_0^\mathrm{T}\boldsymbol{v} - u_0 = 0, \tag{73}$$

where the constraint of the voltage source has been added as an additional equation. The notations

$$\gamma := W^{\mathrm{T}} v + \hat{w}, \quad \hat{w} := \begin{pmatrix} 0 \\ a \end{pmatrix} \tag{74}$$

and relation (3) are used to formulate the measure inclusions of the ideal diode and the unilateral switch as complementarity conditions

$$\mathbf{0} \preceq \gamma^+ \perp \mathrm{d}\mathcal{I} \succeq \mathbf{0}, \tag{75}$$

allowing to set up the linear complementarity problem after discretisation. For non-smooth mechanical systems, usually Moreau's midpoint rule is used to discretise the measure differential inclusions. Moreau's midpoint rule consists of a trapezoidal rule for the positions and an explicit Euler step for the velocities. For the discretisation of the DC–DC buck converter, an implicit Euler scheme is used, instead of Moreau's midpoint rule. In contrast to the midpoint rule, the implicit Euler scheme does not require a regular capacitor matrix M. Using the implicit Euler scheme, the integral of all measures in Equation (73) are approximated using end-point terms, yielding

$$\begin{aligned}
&\int_{\Delta t} M \, \mathrm{d}v \approx M \int_{\Delta t} \mathrm{d}v = M(v_E - v_A), \\
&\int_{\Delta t} D v \, \mathrm{d}t \approx D v_E \int_{\Delta t} \mathrm{d}t = D v_E \Delta t, \\
&\int_{\Delta t} K q \, \mathrm{d}t \approx K q_E \int_{\Delta t} \mathrm{d}t = K q_E \Delta t, \tag{76} \\
&\int_{\Delta t} W \, \mathrm{d}\mathcal{I} \approx W \int_{\Delta t} \mathrm{d}\mathcal{I} = W \Delta \mathcal{I}, \\
&\int_{\Delta t} w_0 \, \mathrm{d}\mathcal{I}_0 \approx w_0 \int_{\Delta t} \mathrm{d}\mathcal{I}_0 = w_0 \Delta \mathcal{I}_0.
\end{aligned}$$

The relation between the nodal voltages v and the nodal fluxes q can be approximated using one implicit Euler step

$$q_E = q_A + v_E \Delta t. \tag{77}$$

The complementarity conditions (75) are expressed in the discretised form

$$\mathbf{0} \preceq \gamma_E \perp \Delta \mathcal{I} \succeq \mathbf{0}, \tag{78}$$

where the vector of local variables at the end-time t_E,

$$\gamma_E = W^{\mathrm{T}} v_E + \hat{w}_A, \tag{79}$$

is formed using the vector $\hat{w}_A$ at the beginning t_A of the time step. This is done in order to avoid a nonlinear dependence on the unknown nodal voltages v_E, which would lead to a nonlinear complementarity problem. By using the vector $\hat{w}_A$ instead of $\hat{w}_E$, a small time-delay of Δt is inserted into the switch control feedback of the DC–DC buck converter, which seems reasonable from the modelling point of view as well. The integral of the equality of measures (73) may be written as

$$\begin{aligned}
&M(v_E - v_A) + D v_E \Delta t + K q_E \Delta t \\
&\quad - W \Delta \mathcal{I} - w_0 \Delta \mathcal{I}_0 = \mathbf{0}, \tag{80} \\
&w_0^{\mathrm{T}} v_E - u_0 = 0,
\end{aligned}$$

using the approximations (76). Elimination of the end-point nodal fluxes q_E from the equations (80) with the help of Equation (77) yields

$$\begin{aligned}
&(M + D\Delta t + K \Delta t^2) v_E - w_0 \Delta \mathcal{I}_0 - M v_A \\
&\quad + K q_A \Delta t - W \Delta \mathcal{I} = \mathbf{0}, \tag{81} \\
&- w_0^{\mathrm{T}} v_E + u_0 = 0,
\end{aligned}$$

where the terms have already been regrouped for the unknown variables v_E and $\Delta \mathcal{I}_0$. With the definition of the vectors and matrices

$$\begin{aligned}
\nu := \begin{pmatrix} v_E \\ \Delta \mathcal{I}_0 \end{pmatrix}, \quad \hat{M} := \begin{pmatrix} M + D\Delta t + K \Delta t^2 & -w_0 \\ -w_0^{\mathrm{T}} & 0 \end{pmatrix}, \\
\hat{h} := \begin{pmatrix} M v_A - K q_A \Delta t \\ -u_0 \end{pmatrix}, \quad \hat{W} := \begin{pmatrix} W \\ \mathbf{0} \end{pmatrix},
\end{aligned} \tag{82}$$

the notation can be simplified to the modified nodal equations

$$\hat{M} \nu - \hat{h} - \hat{W} \Delta \mathcal{I} = \mathbf{0}, \tag{83}$$

where the unknown vector ν now contains both the end-point nodal voltages v_E and the current impulsion difference $\Delta \mathcal{I}_0$ of the set-valued voltage source branch. Equation (79) can be written as

$$\gamma_E = \hat{W}^{\mathrm{T}} \nu + \hat{w}_A, \tag{84}$$

using the matrix $\hat{W}$ and the vector ν. If the matrix $\hat{M}$ is regular then Equation (83) can be solved for the vector ν and can be inserted into Equation (84). The resulting linear relation between γ_E and $\Delta\mathcal{I}$ forms together with the complementarity condition (78) the linear complementarity problem

$$\underbrace{\gamma_E}_{y} = \underbrace{\hat{W}^{\mathrm{T}}\hat{M}^{-1}\hat{W}}_{A}\underbrace{\Delta\mathcal{I}}_{x} + \underbrace{\hat{W}^{\mathrm{T}}\hat{M}^{-1}\hat{h} + \hat{w}_A}_{b},$$

$$\underbrace{\mathbf{0} \preceq \gamma_E \perp \Delta\mathcal{I} \succeq \mathbf{0}}_{\mathbf{0} \preceq y \perp x \succeq \mathbf{0}} \tag{85}$$

in standard form (cf. Section 2). It has to be noted, that the matrix $\hat{M}$ is regular not only for the extended DC–DC buck converter, but for the original version as well. After solving the linear complementarity problem (85) for the vectors γ_E and $\Delta\mathcal{I}$, the vector ν can be calculated from Equation (83), yielding the end-point nodal voltages v_E. The nodal fluxes q_E can then be calculated with the help of Equation (77).

5.3 The original DC–DC buck converter

In this section, a model with a minimal number of states for the original DC–DC buck converter is derived. The original DC–DC buck converter, as depicted in Fig. 9, is missing the two additional capacitors C^* and C°, which have been added to the circuit in Section 5.2 to assure a regular matrix M of capacitances. For the circuit of the original DC–DC buck converter, as shown in Fig. 13, the same notations as for the extended version are used. The measure differential inclusions of the original buck converter can be obtained from the inclusions of the extended version by setting the capacitors C^* and C°
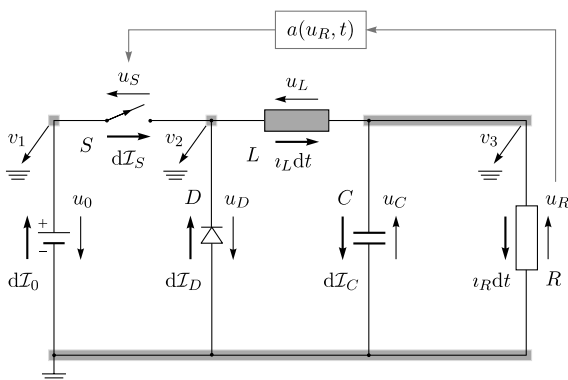

Fig. 13 Electrical model of the original DC–DC buck converter

to zero

$$C^\circ = 0, \quad C^* = 0. \tag{86}$$

Alternatively, one could as well derive the inclusions by formulating the nodal transformation and Kirchhoff's current law directly for the original circuit. By setting a capacity to zero, the according branch relation reduces to

$$\mathrm{d}\mathcal{I} = 0, \quad u \in \mathbb{R}, \tag{87}$$

which is the behaviour of an isolator. For $C^\circ = 0, C^* = 0$, Equations (63) simplify to

$$\mathrm{d}\mathcal{I}_S - \mathrm{d}\mathcal{I}_0 = 0,$$
$$-\frac{1}{L}(q_3 - q_2)\,\mathrm{d}t - \mathrm{d}\mathcal{I}_S - \mathrm{d}\mathcal{I}_D = 0, \quad \dot{q} = v\ \mathrm{d}t\text{-a.e.}$$
$$C\,\mathrm{d}v_3 + \frac{1}{L}(q_3 - q_2)\,\mathrm{d}t + \frac{1}{R}v_3\,\mathrm{d}t = 0. \tag{88}$$

The first equation in Equation (88) is only needed to determine the current impulsion measure $\mathrm{d}\mathcal{I}_0$, and is therefore removed from the set of equations. The set-valued branch relations for the diode, the switch and the voltage source remain the same as for the extended DC–DC buck converter. For the branch relations, one obtains

$$-\mathrm{d}\mathcal{I}_D \in \mathrm{Upr}(v_2^+),$$
$$-\mathrm{d}\mathcal{I}_S \in \mathrm{Upr}(a^+ + v_2^+ - v_1^+), \tag{89}$$
$$-\mathrm{d}\mathcal{I}_0 \in \mathbb{R}, \quad v_1 - u_0 = 0,$$

after inserting the nodal transformation (59) into Equation (64). The states v_1 and q_1 can be eliminated from the system (88), (89) by solving the branch relation of the voltage source for the nodal voltage v_1 and by inserting it into the branch relation of the unilateral switch, yielding

$$-\mathrm{d}\mathcal{I}_D \in \mathrm{Upr}(v_2^+),$$
$$-\mathrm{d}\mathcal{I}_S \in \mathrm{Upr}(a^+ + v_2^+ - u_0). \tag{90}$$

The remaining nodal voltages v_2, v_3 and the associated nodal fluxes q_2, q_3 are replaced with the local variables

$$u_C = -v_3, \quad u_L = v_3 - v_2,$$
$$\varphi_C = -q_3, \quad \varphi_L = q_3 - q_2, \tag{91}$$

which link the states directly with the dynamical elements. The current impulsion measures $d\mathcal{I}_S$ and $d\mathcal{I}_D$ occur in the remaining last two equations of Equation (88) only as a sum, for which the notation

$$d\mathcal{I} := d\mathcal{I}_S + d\mathcal{I}_D \tag{92}$$

is defined. By inserting Equations (91) and (92) into the Equation (88) one obtains

$$-\frac{1}{L}\varphi_L \, dt = d\mathcal{I}, \quad u_L = \dot{\varphi}_L \ dt\text{-a.e.}$$
$$du_C = \frac{1}{LC}\varphi_L \, dt - \frac{1}{RC}u_C \, dt. \tag{93}$$

The current impulsion measure $d\mathcal{I}$ can be expressed by summing the inclusions (90) and replacing the nodal voltage v_2 with the branch voltages u_C and u_L, yielding

$$- d\mathcal{I} \in \mathrm{Upr}(-u_C^+ - u_L^+) + \mathrm{Upr}(a^+ - u_C^+ - u_L^+ - u_0). \tag{94}$$

With the rule for the addition of two unilateral primitives (8), the inclusion (94) can be further simplified to

$$- d\mathcal{I} \in \mathrm{Upr}(-u_C^+ - u_L^+ - b^+), \ b := \max(0, u_0 - a). \tag{95}$$

The switch control a, expressed in the capacitor branch voltage u_C, can be written as

$$a(u_C, t) = \begin{cases} 0, & -u_C \leq h(t), \\ +\infty, & -u_C > h(t). \end{cases} \tag{96}$$

Using Equation (96) and $u_0 > 0$, the max condition in Equation (95) is further simplified, yielding

$$b(u_C, t) = \begin{cases} u_0, & -u_C \leq h(t), \\ 0, & -u_C > h(t). \end{cases} \tag{97}$$

We further introduce a variable s to abbreviate the argument in the Upr-inclusion (95),

$$s := -u_C - u_L - b, \tag{98}$$

to simplify the notation on the one hand and to set up the linear complementarity problem in standard form on the other hand. By using the notation (98) and the Upr inversion rule (4), the inclusion (95) can be transformed to

$$-s^+ \in \mathrm{Upr}(d\mathcal{I}). \tag{99}$$

After eliminating the current impulsion measure $d\mathcal{I}$ with the first equation of Equation (93), the inclusion (99) can be written as

$$-s^+ \in \mathrm{Upr}(-\varphi_L), \tag{100}$$

or as complementarity conditions

$$0 \leq -\varphi_L \perp s^+ \geq 0, \tag{101}$$

if the inductivity L is assumed to be strictly positive. With this complementarity condition, the minimal description of the original DC–DC buck converter is complete. The set of equations which completely determines the system can be written as

$$du_C = \frac{1}{LC}\varphi_L \, dt - \frac{1}{RC}u_C \, dt, \quad u_L = \dot{\varphi}_L \ dt\text{-a.e.}$$
$$s = -u_C - u_L - b, \quad b = \begin{cases} u_0, & -u_C \leq h(t), \\ 0, & -u_C > h(t), \end{cases} \tag{102}$$
$$0 \leq -\varphi_L \perp s^+ \geq 0.$$

The description (73) derived for the extended DC–DC buck converter uses the six states $v_1, v_2, v_3, q_1, q_2, q_3$ and the two complementarity conditions associated with $d\mathcal{I}_D$ and $d\mathcal{I}_S$. Compared to this, the description (102) of the original DC–DC buck converter uses only the two states u_C, φ_L and one complementarity condition. The minimal mechanical model associated with the original DC–DC buck converter can be obtained from Equation (102) by using the position–flux analogy. The model is illustrated in Fig. 14. It consists of a mass C that is connected with a damper $1/R$ to the environment like the extended model. The linear spring with stiffness coefficient $1/L$ connects the mass C to a sprag clutch, which itself acts on a relative velocity constraint $b(u_C, t)$. The velocity $b(u_C, t)$ is a nonlinear function of the velocity u_C of the mass C and the time t. Similar to the extended DC–DC buck converter described in Section 5.2, the time-stepping method and an Euler scheme for discretisation is used to solve the
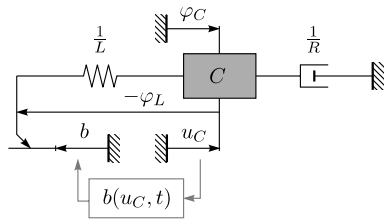
Fig. 14 Mechanical model associated with the original DC–DC buck converter

original DC–DC buck converter numerically. Due to the structure of the system (102), the midpoint rule as used for mechanical systems cannot be applied. The end-time t_E of the considered time-step Δt is calculated as

$$t_E = t_A + \Delta t, \tag{103}$$

where t_A is the beginning of the step. The integral of all measures in the first equation of Equation (102) are approximated using an explicit Euler scheme, yielding

$$
\begin{aligned}
\int_{\Delta t} \mathrm{d}u_C &\approx u_{CE} - u_{CA}, \\
\int_{\Delta t} \frac{1}{LC}\varphi_L \, \mathrm{d}t &\approx \frac{1}{LC}\varphi_{LA}\Delta t, \\
\int_{\Delta t} \frac{1}{RC}u_C \, \mathrm{d}t &\approx \frac{1}{RC}u_{CA}\Delta t,
\end{aligned}
\tag{104}
$$

where an index A denotes terms at the beginning and E at the end of the time interval Δt. Using the approximations (104), one obtains

$$u_{CE} - u_{CA} = \frac{1}{LC}\varphi_{LA}\Delta t - \frac{1}{RC}u_{CA}\Delta t \tag{105}$$

for the discrete form of the first equation of Equation (102). The relation between the inductor voltage u_L and the inductor flux φ_L is approximated using and implicit Euler scheme, yielding

$$\varphi_{LE} = \varphi_{LA} + u_{LE}\Delta t. \tag{106}$$

The complementarity condition of Equations (102) are expressed with the discretised complementarity condition

$$0 \le -\varphi_{LE} \perp s_E \ge 0, \tag{107}$$

where the variable s_E is obtained as

$$s_E = -u_{CE} - u_{LE} - b(u_{CE}, t_E). \tag{108}$$

In the approximations (104) an explicit Euler scheme has been used, in order to avoid the nonlinear dependency of s_E from φ_{LE} in the case of an implicit Euler scheme. In order to set up the linear complementarity problem for the inductor flux φ_{LE}, the inductor voltage u_{LE} is eliminated from Equation (108) using Equation (106). For the linear complementarity problem, one obtains

$$\underbrace{-\varphi_{LE}}_{y} = \underbrace{\Delta t}_{A}\underbrace{s_E}_{x} + \underbrace{u_{CE}\Delta t + b(u_{CE}, t_E)\Delta t - \varphi_{LA}}_{b},$$
$$0 \le \underbrace{-\varphi_{LE}}_{y} \perp \underbrace{s_E}_{x} \ge 0, \tag{109}$$

where the capacitor voltage u_{CE} results from Equation (105) as

$$u_{CE} = u_{CA} + \frac{1}{LC}\varphi_{LA}\Delta t - \frac{1}{RC}u_{CA}\Delta t \tag{110}$$

To solve for an approximation of the state (u_{CE}, φ_{LE}) at the end-time t_E, given the state (u_{CA}, φ_{LA}) at the time t_A, two steps have to be done. First, one calculates the capacitor voltage u_{CE} using Equation (110) and evaluates the function $b(u_{CE}, t_E)$ from Equation (102). In a second step, one has to solve the linear complementarity problem (109), yielding the solution for φ_{LE}. In Table 8, the MATLAB® implementation of the time-stepping algorithm for the original DC–DC buck converter is given. Numerical results are shown in Fig. 15. The results are obtained for the system in a chaotic parameter regime, as published in [11, 13]. The following values have been used for the parameters of the system: $R = 22\,\Omega$, $C = 47\,\mu\text{F}$, $L = 20\,\text{mH}$, $T = 400\,\mu\text{s}$, $u_0 = 35\,\text{V}$, $u_{\text{ref}} = 11.3\,\text{V}$, $u_l = 3.8\,\text{V}$, $u_u = 8.2\,\text{V}$, $K = 8.2$. The states $u_C(0) = -11.7636\,\text{V}$ and $\varphi_L(0) = -10.584\,\text{mWb}$ have been used to initialize the system. In Fig. 15, the comparator voltage u_{comp} and the output voltage $u_g(t)$ of the ramp generator are shown. The unilateral switch S is closed for $u_{\text{comp}} \le u_g(t)$ and open for $u_{\text{comp}} > u_g(t)$. Fig. 15 shows as well the phase space plot of the DC–DC buck converter. The

Table 8 The MATLAB®
implementation of the
time-stepping algorithm for
the original DC-DC buck
converter

```
function [t, u_C, phi_L, u_L, i_L] = orgbuck(u_C0, phi_L0, t_end, dt)

% Parameters
R = 22; C = 4.7e-5; L = 0.02; u_0 = 35;
T = 4.0e-4; u_ref = 11.3; u_l = 3.8; u_u = 8.2; K = 8.2;

% Initial conditions
t_A = 0; t(1) = 0;
u_CA = u_C0; u_C(1) = 0;
phi_LA = phi_L0; phi_L(1) = 0;

i = 0;
while (t_A < t_end)
  t_E = t_A + dt;
  u_CE = u_CA + 1 / (L * C) * phi_LA * dt - 1 / (R * C) * u_CA * dt;
  b_E = b(u_CE, t_E, u_0, u_l, u_u, u_ref, T, K);

  [n_phi_LE, s_E] = lcp(dt, (u_CE + b_E) * dt - phi_LA);
  phi_LE = -n_phi_LE;
  u_LE = -u_CE - b_E - s_E;

  t_A = t_E; u_CA = u_CE; phi_LA = phi_LE; i = i + 1;
  t(i) = t_E; u_C(i) = u_CE; phi_L(i) = phi_LE; u_L(i) = u_LE;
end
i_L = - 1 / L * phi_L;

% ---------------------------------------------------------------------------

function result = b(u_C, t, u_0, u_l, u_u, u_ref, T, K)
h = u_ref + 1 / K * (u_l + mod(t, T) / T * (u_u - u_l));
if -u_C <= h
  result = u_0;
else
  result = 0;
end

% ---------------------------------------------------------------------------

function [y, x] = lcp(A, b)
% scalar LCP with A > 0
if b >= 0
  y = b;
  x = 0;
else
  y = 0;
  x = -b / A;
end
```
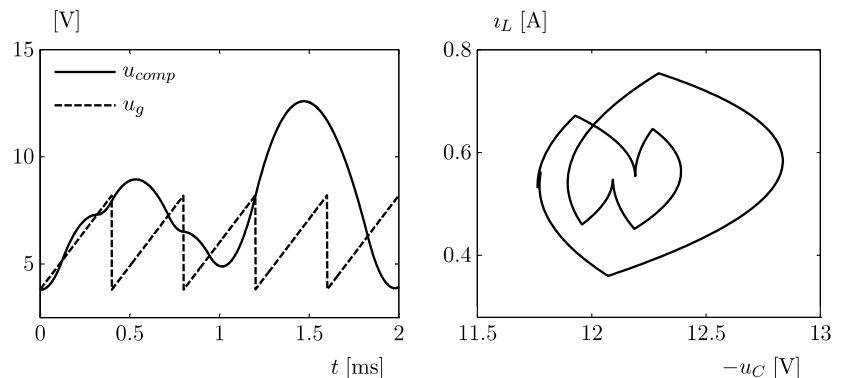
Fig. 15 Phase space plot
and comparator voltages of
the DC–DC buck converter

numerical results agree with those published in [11, 13] and those obtained with a MATLAB® implementation of the extended DC–DC buck converter for $C^\circ = 0$, $C^* = 0$.

6 Conclusion

In this paper, the flux approach has been extended to non-smooth electrical systems. The assumptions and

formulations used for mechanical systems have been adopted for the flux approach using the position–flux analogy. For the most important non-smooth elements, like diodes and switching elements, branch relations have been formulated in the flux approach and related to analogous mechanical elements. Using the example of the DC–DC buck converter, the formulation of the measure differential inclusions and their solution using the time-stepping method has been shown for the flux approach. Only a small set of non-smooth elements have been described in this paper to show the basic procedure. The formulations used are not limited to this set of elements only. There are many semiconductor elements as, for example, Zener diodes that can be modeled with non-smooth set-valued branch relations.

For the capacitor, resistor and inductor, only linear branch relations have been used. With the extension to nonlinear elements, a nonlinear complementarity problem or a set of nonlinear equations can be obtained, if the implicit Euler scheme is used for the discretisation. While the numerical solution of a linear complementarity problem is already a very difficult problem, the solution of a nonlinear complementarity problem is even worse. By using an explicit discretisation scheme, the difficulties of the nonlinear complementarity problem can be avoided, but other problems like numerical stability are added. One possible solution for the implicit case could be the transformation into a set of nonlinear equations using the Augmented Lagrangian approach.

The limitation to continuous charges in the charge approach and to continuous fluxes in the flux approach result in different impact relations for the non-smooth elements in each approach. The combination of the charge approach and the flux approach into a mixed approach, which could overcome these differences, is an area of active research.

References

1. Acary, V., Brogliato, B.: Numerical time integration of higher order dynamical systems with state constraints. In: ENOC-2005, Eindhoven, The Netherlands, August 7–12 (2005)

2. Alart, P., Curnier, A.: A mixed formulation for frictional contact problems prone to Newton like solution methods. Comput. Methods Appl. Mech. Eng. **92**(3), 353–357 (1991)

3. Anitescu, M., Potra, F.A., Stewart, D.E.: Time-stepping for three-dimensional rigid body dynamics. Comput. Methods Appl. Mech. Eng. **177**(3), 183–197 (1999)

4. Banerjee, S., Grebogi, C.: Border collision bifurcations in two-dimensional piecewise smooth maps. Phys. Rev. E **59**(4), 4052–4061 (1999)

5. Banerjee, S., Ott, E., Yorke, J.A., Yuan, G.H.: Anomalous bifurcations in DC–DC converters: borderline collisions in piecewise smooth maps. In: IEEE Power Electronic Specialists Conference, St. Louis, MO, USA, pp. 1337–1344 (1997)

6. Bedrosian, D., Vlach, J.: Time-domain analysis of networks with internally controlled switches. IEEE Trans. Circuits Syst., Part I: Fundam. Theory Appl. **39**(3), 199–212 (1992)

7. Cottle, R.W., Pang, J.S., Stone, R.E.: The Linear Complementarity Problem. Academic, London (1992)

8. Crandall, S.H., Karnopp, D.C., Kurtz, E.F. Jr., Pridmore-Brown, D.C.: Dynamics of Mechanical and Electromechanical Systems. McGraw-Hill, New York (1968)

9. Desoer, Ch.A., Kuh, E.S.: Basic Circuit Theory. McGraw-Hill, Tokyo (1969)

10. Enge, O., Maißer, P.: Modelling electromechanical systems with electrical switching components using the linear complementarity problem. Multibody Syst. Dyn. **13**(4), 421–445 (2005)

11. Fosas, E., Olivar, G.: Study of chaos in the buck converter. Part I: Fundam. Theory Appl. IEEE Trans. Circuits Syst. **43**(1), 13–25 (1996)

12. Glocker, Ch.: Set-valued force laws: Dynamics of Non-Smooth Systems, Vol 1. Lecture Notes in Applied Mechanics. Springer, Berlin (2001)

13. Glocker, Ch.: Models of non-smooth switches in electrical systems. Int. J. Circuit Theory Appl. **33**, 205–234 (2005)

14. Jean, M.: The non-smooth contact dynamics method. Comput. Methods Appl. Mech. Eng. **177**, 235–257 (1999)

15. Mazumder, S.K., Nayfeh, A.H., Boroyevich, D.: Theoretical and experimental investigation of the fast- and slow-scale instabilities of a DC–DC converter. IEEE Trans. Power Electron. **16**(2), 201–216 (2001)

16. Mazumder, S.K., Nayfeh, A.H., Boroyevich, D.: An investigation into the fast- and slow-scale instabilities of a single phase bidirectional boost converter. IEEE Trans. Power Electron. **18**(4), 1063–1069 (2003)

17. Moreau, J.J.: Unilateral contact and dry friction in finite freedom dynamics, vol. 302. CISM Courses and Lectures. Springer-Verlag, Wien, Austria (1988)

18. Ogrodzki, J.: Circuit Simulation Methods and Algorithms. CRC, Boca Raton, FL (1994)

19. Stewart, D.E., Trinkle, J.C.: An implicit time-stepping scheme for rigid body dynamics with inelastic collisions and Coulomb friction. Int. J. Numer. Methods Eng. **39**(15), 2673–2691 (1996)

20. Tse, C.K., Adams, K.M.: Qualitative analysis and control of a DC-to-DC boost converter operating in discontinuous mode. IEEE Trans. Power Electron. **5**(3), 323–330 (1990)